arXiv:astro-ph/0503649v2 31 Mar 2005

On the relation between circular velocity and central velocity dispersion in high and low surface brightness galaxies[1]

A. Pizzella[1], E.M. Corsini[1], E. Dalla Bontà[1], M. Sarzi[2], L. Coccato[1]

and

F. Bertola[1]

ABSTRACT

In order to investigate the correlation between the circular velocity V_c and the central velocity dispersion of the spheroidal component σ_c, we analyzed these quantities for a sample of 40 high surface brightness disc galaxies (hereafter HSB), 8 giant low surface brightness spiral galaxies (hereafter LSB), and 24 elliptical galaxies characterized by flat rotation curves. Galaxies have been selected to have a velocity gradient $\leq$ 2 km s^{-1} kpc^{-1} for $R \geq 0.35R_{25}$. We used these data to better define the previous V_c–σ_c correlation for spiral galaxies (which turned out to be HSB) and elliptical galaxies, especially at the lower end of the σ_c values. We find that the V_c–σ_c relation is described by a linear law out to velocity dispersions as low as $\sigma_c \approx$ 50 km s^{-1}, while in previous works a power law was adopted for galaxies with $\sigma_c >$ 80 km s^{-1}.

Elliptical galaxies with V_c based on dynamical models or directly derived from the H I rotation curves follow the same relation as the HSB galaxies in the V_c–σ_c plane. On the contrary, the LSB galaxies follow a different relation, since most of them show either higher V_c (or lower σ_c) with respect to the HSB galaxies. This argues against the relevance of baryon collapse in the radial density profile of the dark matter haloes of LSB galaxies. Moreover, if the V_c–σ_c relation is equivalent to one between the mass of the dark matter halo and that of the supermassive black hole, these results suggest that the LSB galaxies host a supermassive black hole with a smaller mass compared to HSB galaxies of equal dark matter halo. On the other hand, if the fundamental correlation of SMBH mass is with the halo circular velocity, then LSBs should have larger black hole masses for given bulge dispersion.

Elliptical galaxies with V_c derived from H I data and LSB galaxies were not considered in previous studies.

[1]Dipartimento di Astronomia, Università di Padova, vicolo dell'Osservatorio 2, I-35122 Padova, Italy

[2]Physics Department, University of Oxford, Keble Road, Oxford, OX1 3RH, UK

Subject headings: black hole physics – galaxies: elliptical and lenticular, cD – galaxies: fundamental parameters – galaxies: haloes – galaxies: kinematics and dynamics – galaxies: spirals

1. Introduction

A possible relation between the central velocity dispersion of the spheroidal component (σ_c) and the galaxy circular velocity measured in the flat region of the rotation curve (V_c) was suggested by Whitmore et al. (1979) and Whitmore & Kirshner (1981). By measuring H I line widths they found that $V_c/\sigma_c \sim 1.7$ for a sample of S0 and spiral galaxies. Recently, Ferrarese (2002) proceeded further extending the V_c–σ_c relation to elliptical galaxies. She interpreted the V_c–σ_c relation as suggestive of a correlation between two different galactic components, since σ_c and V_c probe the potential of the spheroidal component and of the dark matter (hereafter DM) halo, respectively. In particular, it results that for a given DM halo the central velocity dispersion of the spheroidal component is independent of the morphological type. The validity of this relation has been confirmed by Baes et al. (2003), who enlarged the sample of spiral galaxies.

For elliptical galaxies, V_c is generally inferred by means of dynamical modelling of the stellar kinematics. This is the case of the giant round and almost non-rotating ellipticals studied by Kronawitter et al. (2000). These galaxies form a unique dynamical family which scales with luminosity and effective radius. As a consequence the maximum circular velocity is correlated to the central velocity dispersion of the galaxy. (Gerhard et al. 2001). Whether the same is true for more flattened and fainter ellipticals is still to be investigated. On the contrary, both shape and amplitude of the rotation curve of a spiral galaxy depend on the galaxy luminosity and morphological type (e.g., Burstein & Rubin 1985; Persic et al. 1996). For this reason for spiral galaxies the V_c–σ_c relation is not expected a priori.

It is interesting to investigate whether the V_c–σ_c relation holds also for less dense objects characterized by a less steep potential well. This is the case of low surface brightness galaxies (hereafter LSB), which are disc galaxies with a central face-on surface brightness $\mu_B \geq 22.6$ mag arcsec^{-2} (e.g., Schombert et al. 1992; Impey et al. 1996). Previous work concentrated on HSB and, to infer the V_c for elliptical galaxies, they relied on stellar dynamical models. In this work we investigated the behavior of elliptical galaxies with HI-based V_c and of LSB

[1]Based on observations made with European Southern Observatory Telescopes at the Paranal Observatory under programmes 67.B-0283, 69.B-0573 and 70.B-0171.

galaxies in the V_c–σ_c relation.

This paper is organized as follows. An overview of the properties of the sample galaxies as well as the analysis of the kinematic data available in literature to derive their V_c and σ_c are presented in Sect. 2. The results and discussion concerning the V_c–σ_c relation are given in Sect. 3.

2. Sample selection

In the past years we started a scientific program aimed at deriving the detailed kinematics of ionized gas and stars in HSB and LSB galaxies in order to study their mass distribution and structural properties. We measured the velocity curves and velocity dispersion profiles along the major axis for both the ionized-gas and stellar components for a preliminary sample of 50 HSB galaxies [10 S0–S0/a galaxies in Corsini et al. (2003); 7 Sa galaxies in Bertola et al. (1996) and Corsini et al. (1999); 16 S0–Sc galaxies in Vega Beltrán et al. (2001); 17 Sb–Scd galaxies in Pizzella et al. (2004b)] and 11 LSB galaxies (Pizzella et al. 2005, 2004a)

The HSB sample consists of disc galaxies with Hubble type ranging from S0 to Scd, an inclination $i \geq 30°$ and a distance $D < 80$ Mpc. The LSB sample consists of disc galaxies with Hubble type ranging from Sa to Irr, an intermediate inclination ($30° \lesssim i < 70°$), and a distance $D < 65$ Mpc (except for ESO 534-G20). Three LSB galaxies, namely ESO 206-G14, ESO 488-G49, and LSBC F563-V02, have been selected from the sample observed by de Blok & McGaugh (1997). The remaining eight objects are LSB galaxies with bulge. They have been selected in Lauberts & Valentijn (1989, hereafter ESO-LV) to have a LSB disc component following the criteria described by Beijersbergen et al. (1999). Due to the bulge light contribution the total central face-on surface brightness of the galaxy could be $\mu_B \leq 22.6$ mag arcsec^{-2}. However, all these objects do have a LSB disc. As far as their total luminosity concerns, LSBC F563-V02 and ESO 488-G49 are two dwarf LSB galaxies but the other nine objects are representative of giant LSB galaxies (e.g., McGaugh et al. 2001).

For all the HSB and LSB galaxies we obtained the ionized-gas rotation curve by folding the observed line-of-sight velocities around the galaxy center and systemic velocity after averaging the contiguous data points and applying a correction for galaxy inclination. We rejected 35 HSB galaxies because they had asymmetric rotation curves or rotation curves which were not characterized by an outer flat portion. Ferrarese (2002) and Baes et al. (2003) considered galaxies with the rotation curve extending farther out than R_{25}. This criterion is not appropriate when the sample galaxies spans a wide range in photometrical properties. For LSB galaxies, which have a lower central surface brightness than HSB galaxies, R_{25}

corresponds to a relatively small radius where the rotation curve may be still rising. For this reason we adopt a criterion that select rotation curves on the basis of their flatness rather then on their extension.

The flatness of each rotation curve has been checked by fitting it with a linear low $V(R) = AR + B$ for $R \geq 0.35R_{25}$. The radial range has been chosen in order to avoid the bulge-dominated region of the rotation curve (e.g., IC 724 and NGC 2815). The rotation curves with $|A| \geq 2$ km s^{-1} kpc^{-1} within 3σ have been considered not to be flat. In this way 15 HSB galaxies and 8 LSB galaxies resulted to have a flat rotation curve. Since the velocity curves of the LSB galaxies were not presented in previous papers, we show their folded rotation curves in Fig. 1. We derived V_c by averaging the outermost values of the flat portion of the rotation curve.

We are therefore confident that we are giving a reliable estimate of the asymptotic value of the circular velocity which traces the mass of the DM halo (see Ferrarese 2002, for a discussion). We derived σ_c from the stellar kinematics by extrapolating the velocity dispersion radial profile to $r = 0''$. This has been done by fitting the 8 innermost data points with an empirical function (either an exponential, or a Gaussian or a constant). We did not apply any aperture correction to σ_c as discussed by Baes et al. (2003), and Pizzella et al. (2004b).

In order to complete our sample of disc galaxies we included all the spiral galaxies previously studied by Ferrarese (2002) and Baes et al. (2003), but which are in addition characterized by a flat rotation curve. We therefore applied to this latter galaxy sample the same flatness criterion applied to our sample .

In summary, we have 23 galaxies (15 HSB and 8 LSB galaxies) from our preliminary sample, 16 spiral galaxies (out of 38) from Ferrarese (2002), and 9 spiral galaxies (out of 12) from Baes et al. (2003). It should be noted that the final sample of HSB galaxies includes 11 early-type objects with Hubble type ranging from S0 to Sab. On the contrary, the sample by Baes et al. (2003) and Ferrarese (2002) was constituted only by late-type spirals with Hubble type Sb or later (except for the Sa NGC 2844).

Finally, we considered a sample of 24 elliptical galaxies with a flat rotation curve and for which both V_c and σ_c are available from the literature. They include 19 objects studied by Kronawitter et al. (2000) who derived V_c by dynamical modeling and 5 objects for which V_c is directly derived from the flat portion of their H I rotation curves. The addition of these last 5 ellipticals is important as it allows to test against model-dependent biases in the $V_c - \sigma_c$ relation.

The V_c of NGC 4278 has been estimated from both the H I rotation curve (Lees 1994,

at a distance from the center of 3.3 R_{25}) and dynamical models (Kronawitter et al. 2000, at a distance from the center of 0.1 R_{25}). The values are in agreement within 2σ error bars. For the further analysis we adopted the H I V_c which has been obtained at a larger distance from the center.

The values σ_c of all the elliptical galaxies have been corrected to the equivalent of an aperture of radius $r_e/8$ following the prescriptions of Jorgensen et al. (1995). The effective radius r_e is taken from de Vaucouleurs et al. (1991, hereafter RC3).

The basic properties of the complete sample of 40 HSB disc galaxies, 8 LSB spiral galaxies and 24 elliptical galaxies are listed in Table 1 as well as their values of V_c and σ_c.

3. Results and discussion

The V_c and σ_c data points of the final sample of galaxies are plotted in Fig. 2. We applied a linear regression analysis to the data by adopting the method by Akritas & Bershady (1996) for bivariate correlated errors and intrinsic scatter (hereafter BCES) both in the $\log V_c$–$\log \sigma_c$ and V_c–σ_c plane. We did not include LSB galaxies in the analysis because they appear to follow a different V_c–σ_c relation as we will discuss later.

Following Ferrarese (2002) and Baes et al. (2003) we fit the function $\log V_c = \alpha \log \sigma_c + \beta$ to the data in $\log V_c$–$\log \sigma_c$ plane. We find

$$\log V_c = (0.74 \pm 0.07)\ \log \sigma_c + (0.80 \pm 0.15) \tag{1}$$

with V_c and σ_c expressed in km s^{-1}. The resulting power law is plotted in Fig. 2. To perform a comparison with previous results we defined the reduced χ^2 as in Press et al. (1992)

$$\chi^2_\nu = \frac{1}{N-2} \sum_{i=1}^{N} \frac{(\log V_{c,i} - \log V^{fit}_{c,i})^2}{\Delta \log V^2_{c,i} + \alpha^2 \Delta \log \sigma^2_{c,i}} \tag{2}$$

where $\Delta \log \sigma_{c,i}$ and $\Delta \log V_{c,i}$ are the errors of the $i-$th data point, $\log V_{c,i}$ and $\log V^{fit}_{c,i}$ are the observed and fitted velocity of the $i-$th data point, $\alpha = 0.74$ is the linear coefficient of the regression, and $N = 64$ is the number of data points. We find $\chi^2_\nu = 2.5$.

The fitting power law has $\alpha \approx 1$ in agreement with Ferrarese (2002) and Baes et al. (2003). The power-law fit by Baes et al. (2003) is plotted in Fig. 2 for a comparison. However, Ferrarese (2002) and Baes et al. (2003) included in their fits only galaxies with $\sigma_c > 70$ km s^{-1} and $\sigma_c > 80$ km s^{-1}, respectively. In fact, they considered the few objects with $\sigma_c \leq 70$ km s^{-1} as outliers. On the contrary, we found that points characterized by $\sigma_c \lesssim 70$

km s^{-1} appear to be well represented by the fitting law as well as the ones characterized by higher values of σ_c.

Since it results $\alpha \approx 1$, we decided to fit the function $V_c = a\sigma_c + b$ to the data in the V_c–σ_c plane. We find

$$V_c = (1.32 \pm 0.09)\,\sigma_c + (46 \pm 14) \tag{3}$$

with V_c and σ_c expressed in km s^{-1}. The resulting straight line is plotted in Fig. 2. We find $\chi^2_\nu = 2.7$ by defining the reduced χ^2 as

$$\chi^2_\nu = \frac{1}{N-2}\sum_{i=1}^{N}\frac{(V_{c,i} - V_{c,i}^{fit})^2}{\Delta V_{c,i}^2 + a^2\Delta\sigma_{c,i}^2} \tag{4}$$

where $\Delta\sigma_{c,i}$ and $\Delta V_{c,i}$ are the errors of the $i-$th data point, $V_{c,i}$ and $V_{c,i}^{fit}$ are the observed and fitted velocity for $i-$th data point, $\alpha = 1.35$ is the linear coefficient of the regression, and $N = 64$ is the number of data points. .

To summarize, in previous works a power law was adopted to describe the correlation between V_c and σ_c for galaxies with $\sigma_c >$ 80 km s^{-1}. We find that data are also consistent with a linear law out to velocity dispersions as low as $\sigma_c \approx$ 50 km s^{-1}. We considered the straight line given in Eq. 3 as reference fit.

Our reduced χ^2 is significantly higher than those found by Ferrarese (2002, $\chi^2_\nu = 0.5$ for a sample of 13 spiral galaxies with $\sigma_c >$ 70 km s^{-1} and 20 elliptical galaxies) and Baes et al. (2003, $\chi^2_\nu = 0.3$ for a sample of 24 spiral galaxies with $\sigma_c >$ 80 km s^{-1}). However, this comparison is affected by the different uncertainties which characterize the V_c and σ_c measurements of the three datasets. In order to allow such a comparison we performed the analysis of the scatter of the data points. We defined the scatter as

$$s = \sqrt{\frac{\sum_{i=1}^{N} d_i^2\, w_i}{\sum_{i=1}^{N} w_i}} \tag{5}$$

with

$$d_i = \frac{a\,\sigma_{c,i} - V_{c,i} + b}{\sqrt{a^2+1}} \tag{6}$$

and

$$w_i = \frac{1}{\Delta\sigma_{c,i}\Delta V_{c,i}} \tag{7}$$

where d_i and w_i are the distance between the $i-$th data point and the straight line of coefficients $a = 1.32$ and $b = 46$ given in Eq. 3 and its weight, respectively. If we consider only the HSB galaxies, the resulting scatter is $s = 11$, 9 and 23 km s^{-1} for Ferrarese (2002), Baes et al. (2003) and our sample, respectively. The difference in the scatter of the datasets

(e.g. $[s(\text{this work})/s(\text{Ferrarese})]^2 = 4.4$) is therefore significantly smaller than the difference of the corresponding χ^2_ν (e.g. $\chi^2_\nu(\text{this work})/\chi^2_\nu(\text{Ferrarese}) = 5.4$). This means that the higher value of our χ^2_ν is mostly due to the smaller error bars than to the larger intrinsic scatter of our HSB+E data points. It should be noticed that Ferrarese (2002) and Baes et al. (2003) considered only galaxies with a flat rotation curve extending at a distance R_{last} larger than the optical radius R_{25}. We relaxed this selection criterion to build our final sample and made sure instead that all rotation curves reached the flat outer parts. The residual plot of Fig. 4 shows that the scatter of the data points corresponding to our sample galaxies with V_c measured at $R_{last} \geq R_{25}$ is comparable to that of the galaxies with V_c measured $R_{last} < R_{25}$. This confirms that this particular scale is not important once the asymptotic part of the rotation curve is reached by the observations. However, Fig. 4 indicates that the residuals are particularly large near $R_{last} \simeq R_{25}$ and that the scatter becomes smaller at $R_{last} > 1.5R_{25}$. In the latter case the flat portion of the rotation curve extends on a larger radial range and therefore V_c is measured with a higher precision. In fact, for $R_{last} \simeq R_{25}$ the scatter increases symmetrically with either $V_c > V_{fit}$ and $V_c < V_{fit}$ values and it indicates that the less extended velocity curves are not introducing any systematic effect. Indeed, the slope of the V_c–σ_c relation that we find is consistent with the one proposed by Ferrarese (2002) and Baes et al. (2003) from a sample of more extended velocity curves.

The measured scatter of the complete sample is $s = 18$ km s^{-1}, which is larger than typical measurement errors for V_c and σ_c ($\simeq$ 10km s^{-1}). For this reason, the measured scatter is dominated by the intrinsic scatter that we estimate to be $\simeq$ 15km s^{-1}.

We investigated the location of the elliptical galaxies with V_c based on H I data and of LSB galaxies in the V_c–σ_c plane. These types of galaxies were not considered by Ferrarese (2002) and Baes et al. (2003).

The data points corresponding to the 5 elliptical galaxies with V_c based on H I data follow the same relation as the remaining disc and elliptical galaxies. For these H I rotation curves we relaxed the flatness criterion in favor of their large radial extension which is about 10 times larger than that of optical rotation curves. The inclusion of these data points does not change the fit based on the remaining disc and elliptical galaxies. They are mostly located on the upper end of the V_c–σ_c relation derived for disc galaxies, in agreement with the findings of Bertola et al. (1993). They studied these elliptical galaxies and showed that their DM content and distribution are similar to those of spiral galaxies.

The LSB and HSB galaxies do not follow the same V_c–σ_c relation. In fact, most of the LSB galaxies are characterized by a higher V_c for a given σ_c (or a lower σ_c for a given V_c) with respect to HSB galaxies (Fig. 2). By applying to the LSB data points the same regression analysis which has been adopted for the HSB and elliptical galaxies of the final

sample, we find

$$V_c = (1.35 \pm 0.19)\,\sigma_c + (81 \pm 23) \tag{8}$$

with V_c and σ_c expressed in km s^{-1}. The straight line corresponding to this fit, which is different from the one obtained for HSB and elliptical galaxies and happens to be parallel to it, is plotted in Fig. 2.

To address the significance of this result, which is based only on 8 data points, we compared the distribution of the normalized scatter of the LSB galaxies to that of the HSB and elliptical galaxies. We defined normalized scatter of the $i-$th data point as

$$\overline{s_i} = d_i/\Delta_i \tag{9}$$

where d_i is the distance to the straight line of coefficient $a = 1.32$ and $b = 46$ given in Eq. 3 of the $i-$th data point, whose associated error Δ_i is

$$\Delta_i = \sqrt{\Delta V_{c,i} \Delta \sigma_{c,i}}. \tag{10}$$

We assumed $\overline{s_i} > 0$ when the data point lies above the straight line corresponding to the best fit. In Fig. 3 we plot the distributions of the normalized scatter of the LSB galaxies and of the HSB and elliptical galaxies. The two distributions appear to be different, as it is confirmed at a high confidence level ($> 99\%$) by a Kolmogorov-Smirnov test. The fact that these objects fall in a different region of the V_c–σ_c plane confirms that LSB and HSB galaxies constitute two different classes of galaxies.

Both demographics of supermassive black holes (SMBH) and study of DM distribution in galactic nuclei benefit from the V_c–σ_c relation. The recent finding that the mass of SMBHs correlates with different properties of the host spheroid supports the idea that formation and accretion of SMBHs are closely linked to the formation and evolution of their host galaxy. Such a mutual influence substantiates the notion of coevolution of galaxies and SMBHs (see Ho 2004).

A task to be pursued is to obtain a firm description of all these relationships spanning a wide range of SMBH masses and address if they hold for all Hubble types. In fact, the current demography of SMBHs suffers of important biases, related to the limited sampling over the different basic properties of their host galaxies. The finding that the V_c–σ_c relation holds for small values of σ_c points to the idea that SMBHs with masses smaller than about 10^6 M$_\odot$ may also exist and follow the M$_\bullet$-σ relation.

Moreover, it has been suggested that the V_c–σ_c relation is equivalent to one between the masses of SMBH and DM halo (Ferrarese & Merritt 2000; Baes et al. 2003) because σ_c and V_c are related to the masses of the central SMBH and DM halo, respectively. Yet, this claim

is to be considered with caution, as the demography of SMBHs is still limited, in particular as far as spiral galaxies are concerned. Furthermore, the calculation of the virial mass of the DM halo from the measured V_c depends on the assumptions made for the DM density profile and the resulting rotation curve (e.g., see the prescriptions by Bullock et al. 2001; Seljak 2002). A better estimate of the virial velocity of the DM halo V_{vir} can be obtained by constraining the baryonic-to-dark matter fraction with detailed dynamical modeling of the sample galaxies. The resulting $V_{vir}-\sigma_c$ relation is expected to have a smaller scatter than the $V_c-\sigma_c$ relation. If the $M_\bullet$-σ relation is to hold, the deviation of LSB galaxies *with bulge* from the $V_c-\sigma_c$ of HSB and elliptical galaxies suggests that for a given DM halo mass the LSB galaxies would host a SMBH with a smaller mass compared to HSB galaxies. On the other hand, if the fundamental correlation of SMBH mass is with the halo circular velocity, then LSBs should have larger black-hole masses for given bulge dispersion. The theoretical and numerical investigations of the processes leading to the formation of LSB galaxies this should be accounted for

The collapse of baryonic matter can induce a further concentration in the DM distribution (Rix et al. 1997), and a deepening of the overall gravitational well in the central regions. If this is the case, the finding that at a given DM mass (as traced by V_c) the central σ_c of LSB galaxies is smaller than in their HSB counterparts, would argue against the relevance of baryon collapse in the radial density profile of DM in LSB galaxies. Confirming that LSB galaxies follow a different $V_c-\sigma_c$ relation will highlight yet another aspect of their different formation history. Indeed, LSB galaxies appear to have a central potential well less steep than HSB spirals of the same DM halo mass. If the collapse of baryonic matter causes a compression of the DM halo as well, for LSB galaxies such process may have been less relevant than for HSB galaxies. Again LSB galaxies turn out to be the best tracers of the primordial density profile of DM haloes and therefore in pursuing the nature of dark matter itself.

We are indebted to Matthew Bershady for providing us the BCES code, which was used to analyze the data. We wish to thank Maarten Baes and Laura Ferrarese for stimulating discussion. This research has made use of the Lyon-Meudon Extragalactic Database (LEDA) and of the NASA/IPAC Extragalactic Database (NED).

REFERENCES

Akritas, M. G., & Bershady, M. A. 1996, ApJ, 470, 706

Baes, M., Buyle, P., Hau, G. K. T., & Dejonghe, H. 2003, MNRAS, 341, L44

Barth, A. J., Ho, L. C., & Sargent, W. L. W. 2002, AJ, 124, 2607

Beijersbergen, M., de Blok, W. J. G., & van der Hulst, J. M. 1999, A&A, 351, 903

Bertola, F., Cinzano, P., Corsini, E. M., Pizzella, A., Persic, M., & Salucci, P. 1996, ApJ, 458, L67

Bertola, F., Pizzella, A., Persic, M., & Salucci, P. 1993, ApJ, 416, L45

Beuing, J., Bender, R., Mendes de Oliveira, C., Thomas, D., & Maraston, C. 2002, A&A, 395, 431

Bullock, J. S., Kolatt, T. S., Sigad, Y., Somerville, R. S., Kravtsov, A. V., Klypin, A. A., Primack, J. R., & Dekel, A. 2001, MNRAS, 321, 559

Burstein, D., & Rubin, V. C. 1985, ApJ, 297, 423

Carollo, C. M., Danziger, I. J., & Buson, L. 1993, MNRAS, 265, 553

Corsini, E. M., Pizzella, A., Coccato, L., & Bertola, F. 2003, A&A, 408, 873

Corsini, E. M., Pizzella, A., Sarzi, M., Cinzano, P., Vega Beltrán, J. C., Funes, J. G., Bertola, F., Persic, M., & Salucci, P. 1999, A&A, 342, 671

Davies, R. L., Burstein, D., Dressler, A., Faber, S. M., Lynden-Bell, D., Terlevich, R. J., & Wegner, G. 1987, ApJS, 64, 581

de Blok, W. J. G., & McGaugh, S. S. 1997, MNRAS, 290, 533

Ferrarese, L. 2002, ApJ, 578, 90

Ferrarese, L., & Merritt, D. 2000, ApJ, 539, L9

Franx, M., van Gorkom, J. H., & de Zeeuw, T. 1994, ApJ, 436, 642

Gerhard, O., Kronawitter, A., Saglia, R. P., & Bender, R. 2001, AJ, 121, 1936

Guthrie, B. N. G. 1992, A&AS, 93, 255

Ho, L. C., ed. 2004, Coevolution of Black Holes and Galaxies

Impey, C. D., Sprayberry, D., Irwin, M. J., & Bothun, G. D. 1996, ApJS, 105, 209

Jorgensen, I., Franx, M., & Kjaergaard, P. 1995, MNRAS, 276, 1341

Kim, D.-W., Jura, M., Guhathakurta, P., Knapp, G. R., & van Gorkom, J. H. 1988, ApJ, 330, 684

Kronawitter, A., Saglia, R. P., Gerhard, O., & Bender, R. 2000, A&AS, 144, 53

Lees, J. F. 1994, in Mass-Transfer Induced Activity in Galaxies, proceedings of the Conference held at the University of Kentucky, Lexington, April 26-30, 1993. Edited by Isaac Shlosman. Cambridge: Cambridge University Press, 1994, 432

McGaugh, S. S., Rubin, V. C., & de Blok, W. J. G. 2001, AJ, 122, 2381

Morganti, R., Sadler, E. M., Oosterloo, T., Pizzella, A., & Bertola, F. 1997, AJ, 113, 937

Palunas, P., & Williams, T. B. 2000, AJ, 120, 2884

Persic, M., Salucci, P., & Stel, F. 1996, MNRAS, 281, 27

Pizzella, A., Corsini, E., Magorrian, J., Sarzi, M., & Bertola, F. 2005, in preparation

Pizzella, A., Corsini, E. M., Bertola, F., Coccato, L., Magorrian, J., Sarzi, M., & Funes, J. G. 2004a, in IAU Symposium, 337–338

Pizzella, A., Corsini, E. M., Vega Beltrán, J. C., & Bertola, F. 2004b, A&A, 424, 447

Press, W. H., Teukolsky, S. A., Vetterling, W. T., & Flannery, B. P. 1992, Numerical recipes in FORTRAN. The art of scientific computing (Cambridge: University Press, —c1992, 2nd ed.)

Rix, H., de Zeeuw, P. T., Cretton, N., van der Marel, R. P., & Carollo, C. M. 1997, ApJ, 488, 702

Rubin, V. C., Burstein, D., Ford, W. K., & Thonnard, N. 1985, ApJ, 289, 81

Sandage, A., & Tammann, G. A. 1981, in Carnegie Inst. of Washington, Publ. 635; Vol. 0; Page 0, 0

Schiminovich, D., van Gorkom, J. H., van der Hulst, J. M., & Malin, D. F. 1995, ApJ, 444, L77

Schombert, J. M., Bothun, G. D., Schneider, S. E., & McGaugh, S. S. 1992, AJ, 103, 1107

Seljak, U. 2002, MNRAS, 334, 797

Vega Beltrán, J. C., Pizzella, A., Corsini, E. M., Funes, J. G., Zeilinger, W. W., Beckman, J. E., & Bertola, F. 2001, A&A, 374, 394

Whitmore, B. C., & Kirshner, R. P. 1981, ApJ, 250, 43

Whitmore, B. C., Schechter, P. L., & Kirshner, R. P. 1979, ApJ, 234, 68

This preprint was prepared with the AAS LaTeX macros v5.2.

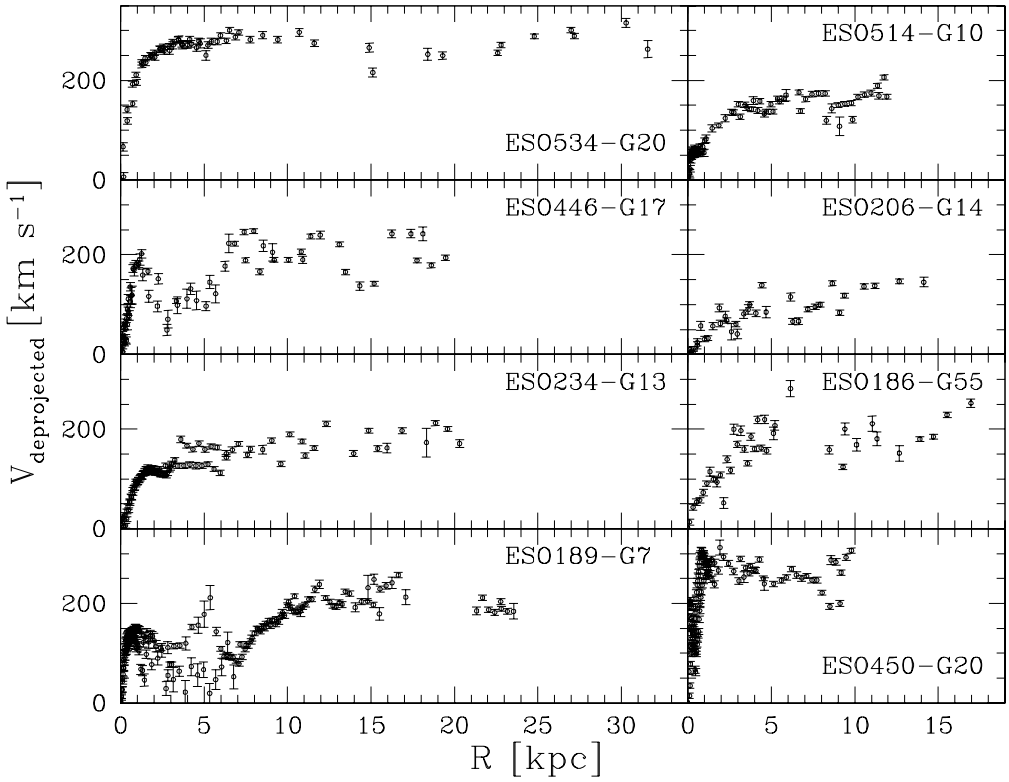

Fig. 1.— Deprojected rotation curves of the eight LSB galaxies of the final sample.

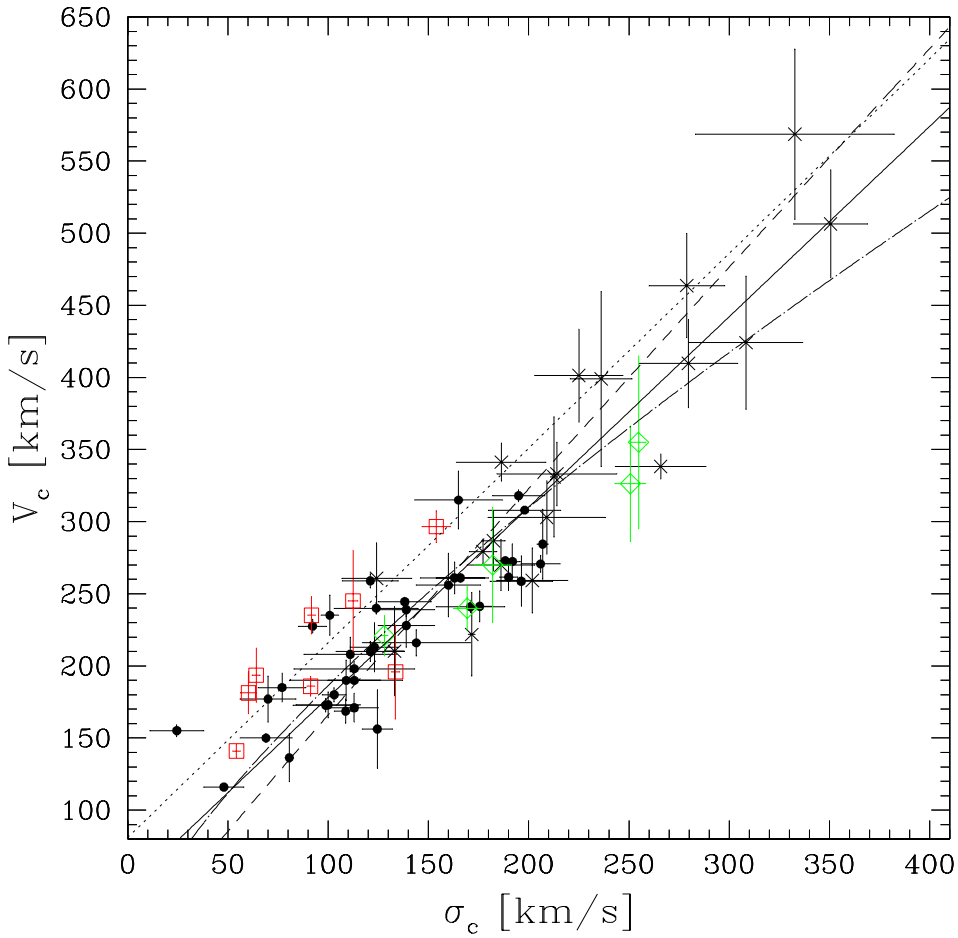

Fig. 2.— The correlation between the circular velocity V_c and the central velocity dispersion of the spheroidal component σ_c for elliptical and disc galaxies. The data points corresponding to HSB galaxies (*filled circles*), LSB galaxies (*squares*), elliptical galaxies with V_c obtained from H I data (*diamonds*), and elliptical galaxies with V_c obtained from dynamical models (*crosses*) are shown. The *continuous* and *dash-dotted line* represent the linear (Eq. 3) and power-law fit (Eq. 1) to HSB and elliptical galaxies. The *dotted line* represents the linear-law fit (Eq. 8) to LSB galaxies. For a comparison, the *dashed line* corresponds to the power-law fit to spiral galaxies with $\sigma_c > 80$ km s^{-1} by Baes et al. (2003).

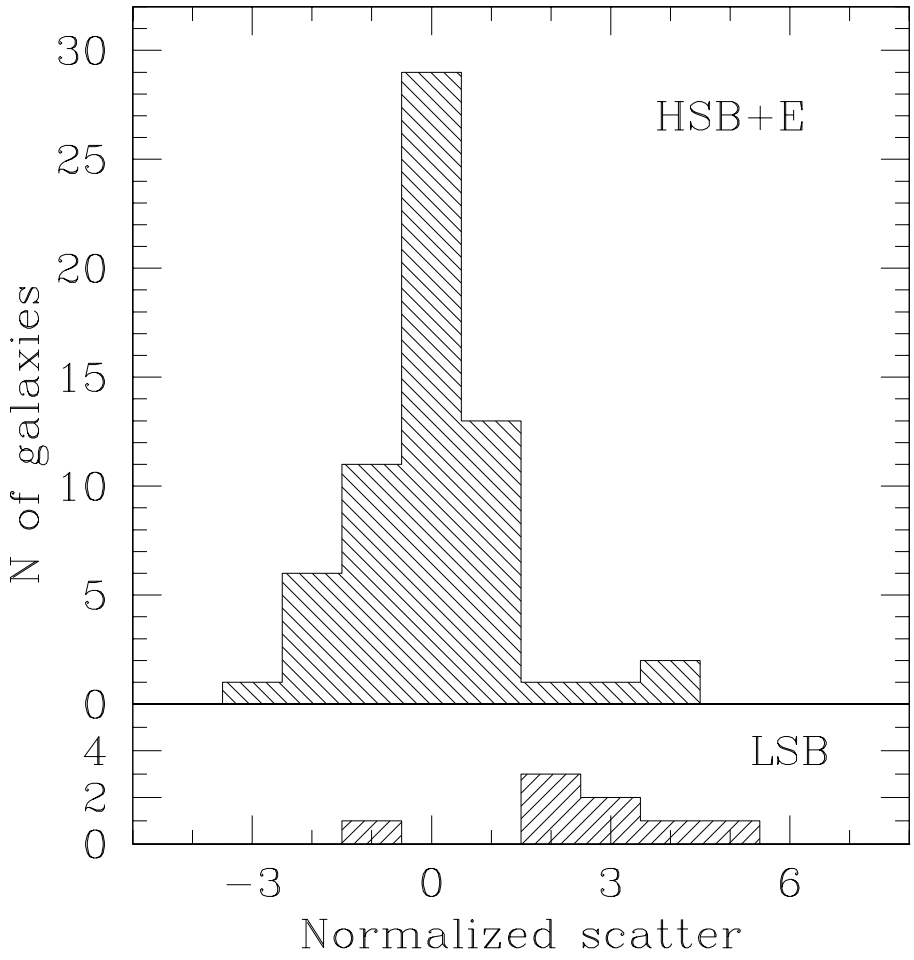

Fig. 3.— The distribution of the normalized scatter of the HSB and elliptical galaxies (*upper panel*) and LSB galaxies (*lower panel*) with respect to the linear-law fit to HSB and elliptical galaxies (Eq. 3). The two distributions are different at $> 99\%$ confidence level.

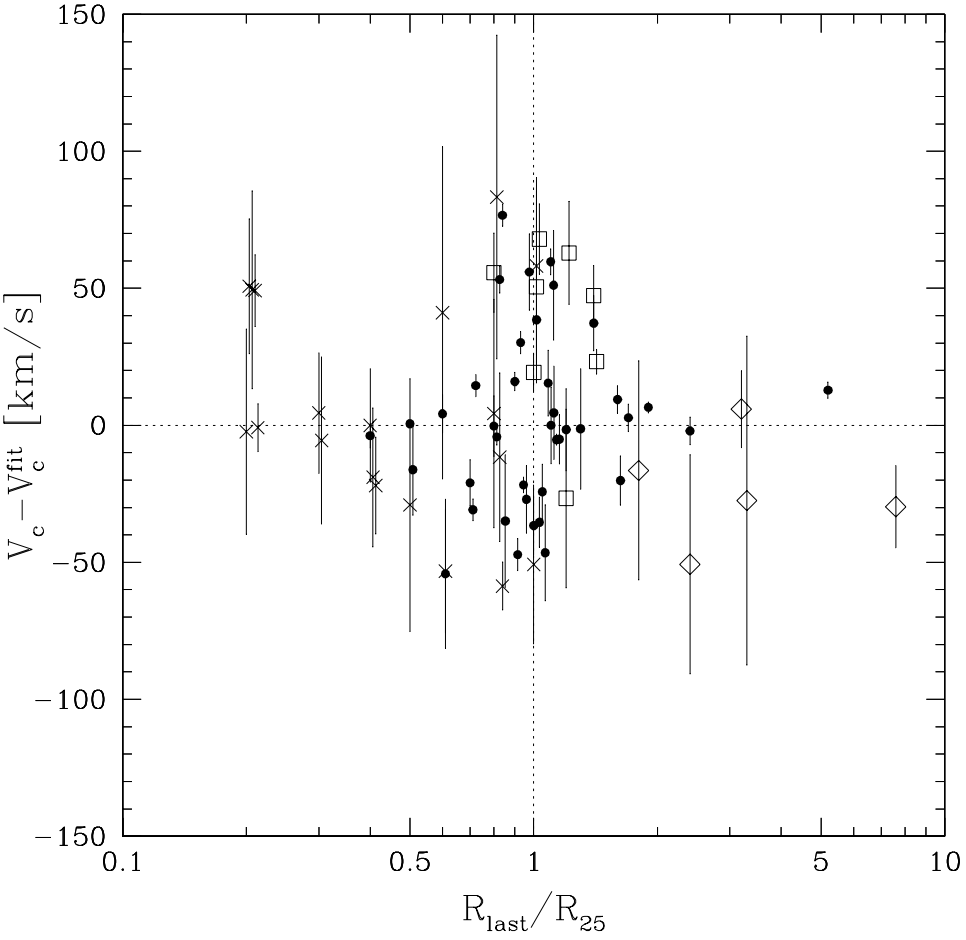

Fig. 4.— Residuals from the linear-law fit to HSB and elliptical galaxies (Eq. 3) plotted as function of R_{last}/R_{25}. The data points corresponding to HSB galaxies (*filled circles*), LSB galaxies (*squares*), elliptical galaxies with V_c obtained from H I data (*diamonds*), and elliptical galaxies with V_c obtained from dynamical models (*crosses*) are shown. Data with the same R_{last}/R_{25} have been shifted to allow comparison.

Table 1: Galaxy Sample

Name	Morp. Type	i	D	$M^0_{B_T}$	σ_c	V_c	R_{last}	Ref.
		[°]	[Mpc]	[mag]	[km s^{-1}]	[km s^{-1}]	[R_{25}]	
(1)	(2)	(3)	(4)	(5)	(6)	(7)	(8)	(9)
HSB galaxies								
ESO 323-G25	(R′)SBbc(s):	55	59.8	−21.2	139 ± 14	228 ± 15	1.2	1
ESO 382-G58	SBbc(r): sp	79	106.2	−22.2	165 ± 22	315 ± 20	1.1	1
ESO 383-G02	SABc(rs)	60	85.4	−21.1	109 ± 28	190 ± 14	1.0	1
ESO 383-G88	SABbc(r)?	67	59.5	−20.6	70 ± 14	177 ± 16	1.0	1
ESO 445-G15	Sbc	66	60.3	−20.2	113 ± 13	190 ± 21	1.1	1
ESO 446-G01	SAbc(s):	53	98.3	−21.4	123 ± 12	213 ± 17	1.0	1
ESO 501-G68	Sbc	70	45.8	−20.1	100 ± 16	173.0 ± 9.0	1.1	1
IC 342	SABcd(rs)	12	2.0	−20.5	77 ± 12	185 ± 10	1.4	2
IC 724	Sa	55	78.0	−21.6	207.0 ± 2.8	284 ± 24	0.8	3
NGC 753	SABbc(rs)	39	90.0	−22.4	121 ± 17	210.0 ± 7.0	0.6	2
NGC 801	Sc	79	79.2	−21.9	144 ± 27	216.0 ± 9.0	1.6	2
NGC 1160	Scd:	62	36.6	−21.0	25 ± 13	155.1 ± 4.0	0.8	4
NGC 1357	SAab(s)	47	26.2	−20.0	121 ± 14	259.0 ± 5.0	0.8	2
NGC 1620	SABbc(rs)	71	46.1	−21.1	92.2 ± 6.9	227.5 ± 4.7	1.1	5
NGC 2179	SA0/a(s)	47	35.6	−19.9	175.6 ± 6.5	241 ± 11	1.0	3
NGC 2590	SAbc(s):	72	63.4	−21.0	196 ± 16	259 ± 18	1.0	5
NGC 2639	(R)SAa(r)?	53	66.5	−21.9	195 ± 13	318.0 ± 4.0	0.7	2
NGC 2815	SBb(r):	72	40.0	−21.6	205.9 ± 9.8	270.7 ± 5.8	0.9	5
NGC 2844	SAa(r):	61	26.4	−18.9	113 ± 12	171 ± 10	1.0	2
NGC 2998	SABc(rs)	63	67.4	−21.6	113 ± 30	198.0 ± 5.0	1.7	2
NGC 3054	SABb(r)	52	28.5	−20.3	138 ± 13	244.5 ± 3.3	0.9	5
NGC 3038	SAb(rs)	58	41.4	−21.5	160 ± 16	256 ± 22	1.3	1
NGC 3145	SBbc(rs)	60	61.0	−22.1	166 ± 12	261.0 ± 3.0	0.8	2
NGC 3198	SBc(rs)	68	9.4	−19.7	69 ± 13	150.0 ± 3.0	5.2	2
NGC 3200	SABc(rs):	73	43.4	−21.5	191.9 ± 3.9	272 ± 12	0.9	5
NGC 3223	SAb(s)	53	46.5	−22.4	163 ± 17	261 ± 11	0.8	2
NGC 3333	SABbc pec sp	82	59.4	−21.3	111 ± 23	208 ± 12	1.0	1
NGC 3885	SA0/a(s)	67	22.3	−19.4	124.5 ± 7.5	156 ± 27	0.6	6
NGC 4378	(R)SAa(s)	21	43.1	−21.0	198 ± 18	308.0 ± 1.0	0.5	2
NGC 4419	SBa(s) sp	71	17.0	−19.6	99 ± 16	172.7 ± 4.5	0.4	4
NGC 4845	SAab(s) sp	76	13.1	−19.2	80.6 ± 2.1	136 ± 17	0.5	3
NGC 5055	SAbc(rs)	55	8.0	−20.5	103.0 ± 6.0	180.0 ± 5.0	2.4	2
NGC 5064	(R′)SAab:	63	36.0	−21.1	188.3 ± 4.6	272.9 ± 2.8	0.9	4
NGC 6503	SAcd(s)	71	5.9	−18.7	48 ± 10	116.0 ± 2.0	1.9	2
NGC 6925	SAbc(s)	75	37.7	−21.9	190.0 ± 4.5	261.5 ± 9.1	1.0	5
NGC 7083	SAbc(s)	53	39.7	−21.5	100.8 ± 4.4	235 ± 14	0.9	5
NGC 7217	(R)SAab(r)	34	21.9	−21.2	171 ± 17	241.0 ± 4.0	0.7	2
NGC 7331	SAb(s)	70	14.9	−21.5	139 ± 14	239.0 ± 5.0	1.6	2
NGC 7531	SABbc(r)	67	20.9	−20.2	108.7 ± 5.6	168.6 ± 8.4	0.7	5
NGC 7606	SAb(s)	67	42.1	−22.2	124 ± 21	240.0 ± 4.0	0.9	2

Note. — Parameters of the final sample of galaxies. The columns show the following: (2) morphological classification from RC3 for HSB and elliptical galaxies and from ESO-LV for LSB galaxies, except for ESO 534-G20 (NED); (3) disc inclination derived for spirals as $\cos^2 i = (q^2 - q_0^2)/(1 - q_0^2)$. The observed axial ratio $q = a/b$ is taken from RC3 and ESO-LV for HSB and LSB galaxies, respectively, except for ESO 446-G17 (Palunas & Williams 2000), ESO 206-G14 (McGaugh et al. 2001), IC 724 (Rubin et al. 1985), and galaxies from Baes et al. (2003) for which we adopted their inclination. The intrinsic flattening $q_0 = 0.11$ is assumed following Guthrie (1992). For ellipticals with H I data the inclination is taken from papers listed in column 9; (4) distance either from papers listed in (10) or derived as V_0/H_0 with $H_0 = 75$ km s^{-1} Mpc^{-1} and V_0 the systemic velocity corrected for the motion of the Sun with respect to the Local Group as in Sandage & Tammann (1981); (5) absolute total blue magnitude from B_T corrected for inclination and extinction from RC3 for HSB and elliptical galaxies and from ESO-LV for LSB galaxies; (6) central velocity dispersion of the

Table 1: (continued)

Name	Morp. Type	i	D	$M^0_{B_T}$	σ_c	V_c	R_{last}	Ref.
		[°]	[Mpc]	[mag]	[km s^{-1}]	[km s^{-1}]	[R_{25}]	
(1)	(2)	(3)	(4)	(5)	(6)	(7)	(8)	(9)
LSB galaxies								
ESO 186-G55	Sab(r)?	63	60.1	−19.1	91.7 ± 2.0	235 ± 11	1.0	7
ESO 189-G07	SABbc(rs)	49	37.5	−20.2	91.3 ± 2.0	185.9 ± 6.9	1.0	7
ESO 206-G14	SABc(s)	39	60.5	−19.0	54.3 ± 2.0	141.0 ± 4.5	1.4	7
ESO 234-G13	Sbc	69	60.9	−19.3	64.1 ± 2.0	194 ± 19	1.2	7
ESO 446-G17	(R)SBb(s)	54	58.9	−20.3	133.6 ± 2.0	196 ± 33	1.2	7
ESO 450-G20	SBbc(s):	30	31.6	−19.5	112.4 ± 2.4	245 ± 35	1.0	7
ESO 514-G10	SABc(s):	36	40.4	−20.2	60.2 ± 4.0	181 ± 15	0.8	7
ESO 534-G20	Sa:	46	226.7	−20.7	153.9 ± 7.1	297 ± 11	1.4	7
Ellipticals with V_c from HI data								
IC 2006	(R)SA0$^-$	31	16.7	−18.9	128.0 ± 1.7	221 ± 14	2.4	8,9
NGC 2865	E3-4	65	31.2	−20.3	169.4 ± 7.0	240 ± 15	3.2	10,11
NGC 2974	E4	55	24.0	−20.2	254.8 ± 3.8	355 ± 60	1.8	12,8
NGC 4278	E1-2	45	7.9	−18.5	250.7 ± 7.7	326 ± 40	3.3	13,14
NGC 5266	SA0$^-$:	63	37.1	−21.4	182.1 ± 9.3	270 ± 40	7.6	15,16
Ellipticals with V_c from dynamical models								
NGC 315	E$^+$:		69.3	−22.3	333 ± 50	569 ± 59	0.8	17,18
NGC 1399	E1 pec		18.1	−20.9	308 ± 28	424 ± 46	0.5	17,18
NGC 2434	E0-1		14.9	−19.3	212.6 ± 1.7	331 ± 42	0.8	17,18
NGC 3193	E2		17.3	−19.5	209 ± 29	303 ± 25	0.4	17,18
NGC 3379	E1		10.1	−19.8	202 ± 18	259 ± 23	0.6	17,18
NGC 3640	E3		15.2	−19.7	177.2 ± 6.8	279.2 ± 8.7	0.2	17,18
NGC 4168	E2		28.9	−20.2	182.4 ± 5.8	287 ± 21	0.4	17,18
NGC 4278	E1-2		7.9	−18.5	250.7 ± 7.7	416 ± 13	0.1	13,18
NGC 4374	E1		12.2	−20.4	280 ± 25	410 ± 31	0.3	17,18
NGC 4472	E2		11.3	−20.9	279 ± 19	464 ± 36	0.2	17,18
NGC 4486	E$^+$0-1 pec		15.5	−21.5	351 ± 19	507 ± 38	0.2	17,18
NGC 4494	E1-2		17.0	−20.6	124 ± 17	261 ± 25	0.2	17,18
NGC 4589	E2		28.9	−20.6	214 ± 30	333 ± 22	0.3	17,18
NGC 4636	E0-1		10.3	−19.6	186 ± 22	341 ± 13	0.2	17,18
NGC 5846	E0-1		21.8	−20.8	266 ± 23	338.3 ± 8.8	0.8	17,18
NGC 6703	SA0$^-$		34.7	−20.7	171.6 ± 1.6	222 ± 29	1.0	17,18
NGC 7145	E0		24.5	−19.9	133.1 ± 4.8	210 ± 31	0.8	17,18
NGC 7192	E$^+$:		36.8	−20.6	186 ± 17	270 ± 18	0.4	17,18
NGC 7507	E0		21.6	−20.4	236 ± 15	399 ± 61	0.6	17,18
NGC 7626	E pec:		48.6	−21.4	225 ± 22	401 ± 32	1.0	17,18

References. — 1: Baes et al. (2003), 2: original references can be found in Ferrarese (2002), 3: Corsini et al. (1999), 4: Vega Beltrán et al. (2001), 5: Pizzella et al. (2004b), 6: Corsini et al. (2003), 7: Pizzella et al. (2005), 8: Kim et al. (1988), 9: Franx et al. (1994), 10: Jorgensen et al. (1995), 11: Schiminovich et al. (1995), 12: Beuing et al. (2002), 13: Barth et al. (2002), 14: Lees (1994), 15: Carollo et al. (1993), 16: Morganti et al. (1997), 17: Davies et al. (1987), 18: Kronawitter et al. (2000).